MHD Rotating flow of Nanofluid over a Semi-infinite vertical moving plate with Constant heat source

Ch. H.K. Gopal

Associate Professor, Department of Mathematics, RVR & JC College of Engineering, Guntur – 522019, Andhra Pradesh - 522019, India.
(Afflicted to Acharya Nagarjuna University, Guntur, AP, India)
Email: krishnagopalch@gmail.com

Abstract

The combined effects of diffusion thermo and radiation absorption on magnetohydrodynamic (MHD) free convective rotating flow of nano-fluids past a semi-infinite permeable moving plate with constant heat source are discussed. Making use of Perturbation technique, we find velocity, temperature and concentration and are examined through graphs. Also, we evaluated the skin friction, Nusselt number and Sherwood number analytically and computationally discussed.

Keywords: Dufour effect, MHD flows, Nanofluid, Radiation-absorption, Porous medium

Nomenclature:

u, v, w	velocity components along x, y and z axes (m/s)
B_0	Applied magnetic field (Wb m^{-2})
C_p	Specific heat (J kg^{-1} K^{-1})
q	complex velocity (m/s)
t	time (s)
T	Local temperature of the nanofluid (K)
T_w	Wall temperature (K)
T_∞	Temperature of the ambient nanofluid (K)
U_0	Characteristic velocity (m s^{-1})
W_0	Mass flux velocity
C	Concentration (kgm^{-3})
C_∞	Concentration in the free stream (kgm^{-3})
g	acceleration due to gravity (m s^{-2})
k	permeability porous medium.
T	temperature of the nanofluid (K),
Q	heat source parameter

β_{nf}	coefficient of thermal expansion of nanofluid (K^{-1})
σ	electric conductivity of the fluid(m^2s^{-1}),
ρ_{nf}	density of the nanofluid (Kg m^{-3})
μ_{nf}	viscosity of the nanofluid (Pa s)
$(\rho C_\rho)_{nf}$	heat capacitance of the nanofluid (J K^{-1}),
α_{nf}	thermal diffusivity of the nanofluid (m^2s^{-1}),
ϕ	solid volume fraction of the nanoparticles,
K_{nf}	thermal conductivity of the nano fluid (m^2 s^{-1})
K_s	thermal conductivity of the solid (m^2 s^{-1})
Q	additional heat source (kJ s^{-1})
β_f	coefficient of thermal expansion of the fluid (K^{-1})
β_C	coefficient of thermal expansion of the solid (K^{-1})
ρ_f	density of the fluid (Kg m^{-3})
ρ_C	density of the solid fractions (Kg m^{-3})
α_{nf}	thermal diffusivity of the nanofluid (m^2s^{-1}),
Ω	constant angular velocity
R	Rotation parameter
Pr	Prandtl number,
S	suction (S>0) or injection (S<0) parameter,
M	Hartmann number
Q_L	radiation absorption parameter,
Kr	chemical reaction parameter,
Sc	Schmidt number,
Gr	Thermal Grashof number,
K	permeability parameter,
Du	diffusion-thermo parameter
Nu	Nusselt number
Sh	Sherwood number
Subscripts	
f	Fluid
s	Solid
nf	Nanofluid

1. Introduction:

The solid particles utilized for nano-fluid is metallic solids *viz.* copper, silver and gold; non-metallic solids *viz.* Titanium oxide, Silica, alumina etc. and metallic liquid *viz.* sodium. The nano-fluid theory was first introduced and had been a field of fluid dynamics by Choi [1]. Recently Ablel-Rahman [2] studied MHD effect and mass transfer flow through a porous medium. The thermal and mass diffusion on MHD flow with Ohmic heating was discussed by Reddy. et al.[3]. Sharma et al. [4] investigated radiation effects on MHD flow past an accelerated vertical plate. Ahmed and Batin [5] discussed MHD flow through porous media with combined effects of induced magnetic field and viscous dissipation. Mutuku-Njane and Makinde [6] investigated on MHD boundary layer flow of nanofluids over a permeable surface with Newtonian heating. The combined effects on an unsteady MHD free convective flow in a vertical channel studied by Krishna et al. [9]. The heat generation/absorption and thermo-diffusion on an unsteady free convective MHD flow near an infinite vertical plate studied by Krishna and Chamkha[10]. Krishna and Chamkha [11] discussed the MHD squeezing flow of a water-based nanofluid between two parallel disks. Krishna and Reddy [14] discussed the unsteady MHD free convection in a boundary layer flow of an electrically conducting fluid through porous medium subject to uniform transverse magnetic field over a moving infinite vertical plate in the presence of heat source and chemical reaction. Krishna and Subba Reddy [15] have investigated the simulation on the MHD forced convective flow through stumpy permeable porous medium. Krishna and Jyothi [16] discussed the Hall effects on MHD Rotating flow of a visco-elastic fluid through a porous medium over an infinite oscillating porous plate with heat source and chemical reaction. Krishna et al. [17] discussed the MHD flow of an electrically conducting second-grade fluid through porous medium over a semi-infinite vertical stretching sheet.

Recently, Krishna et al. [18-21] discussed the MHD flows of an incompressible and electrically conducting fluid in planar channel. Veera Krishna et al. [22] discussed heat and mass transfer on unsteady MHD oscillatory flow of blood through porous arteriole. Sadiq et al. [23] the steady fully developed MHD free convection flow through a porous medium in a micro-channel bounded by two infinite vertical parallel plates due to asymmetric heating of plates taking Hall and ion slip effects into account. Veera Krishna and Chamkha [24] investigated The diffusion-thermo, radiation-absorption and Hall and ion slip effects on MHD free convective rotating flow of nano-fluids (Ag and TiO2) past a semi-infinite permeable moving plate with constant heat source. Veera Krishna et al.[25] discussed the Soret and Joule effects of MHD mixed convective flow of an incompressible and electrically conducting viscous fluid past an infinite vertical porous plate taking Hall effects into account. Veera Krishna and Chamkha [26] discussed the MHD squeezing flow of a water-based nanofluid through a saturated porous medium between two parallel disks, taking the Hall current into account. Hall and ion slip effects on Unsteady MHD Convective Rotating flow of Nanofluids have been discussed by Veera Krishna and Chamkha [27]. Veera Krishna [28] investigated the heat transport on steady MHD flow of copper and alumina nanofluids past a stretching porous surface. Veera Krishna et al.[29] discussed investigated the Hall and ion slip effects on the unsteady MHD free convective rotating flow through porous medium past an exponentially accelerated inclined plate. The combined effects of Hall and ion slip on MHD rotating flow of ciliary propulsion of microscopic organism through porous medium have been studied by Veera Krishna et al.[30]. Veera Krishna and Chamkha [31] investigated the Hall and ion slip effects on the MHD convective flow of elastico-viscous fluid through porous medium between two rigidly rotating parallel plates with time fluctuating sinusoidal pressure gradient. Veera Krishna [32] reported that the Hall and ion slip effects on MHD free convective rotating flow bounded by the semi-infinite vertical porous surface. Veera Krishna [33] discussed the MHD laminar flow of an elastico-viscous electrically conducting Walter's fluid through a circular cylinder or a pipe. In this paper, the combined effects of diffusion thermo and radiation absorption on MHD free convective flow of a nano-fluid past a semi-infinite flat permeable porous plate are analyzed.

2. Formulation and Solution of the problem

We have considered an unsteady MHD convective rotating flow of nano-fluid (Ag and TiO_2) past an infinite vertical permeable moving plate with constant heat source. The physical model is as shown in the Fig. 1. The nano-particles are assumed to have a uniform shape and size. Also both the fluid phase nano-particles are in thermal equilibrium state. Plate is moving infinitely, all the physical variables are functions of z and time t only. The governing equations for the flow are given by.

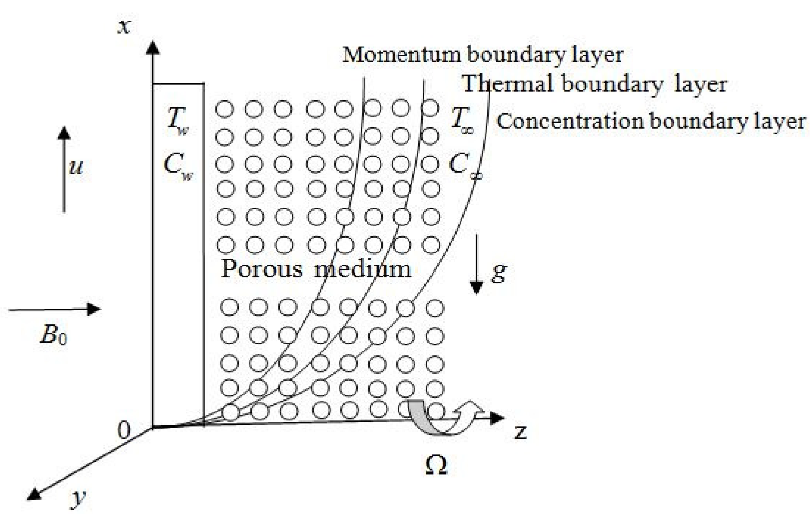

Fig. 1 Physical Configuration of the problem

$$\frac{\partial w}{\partial z} = 0 \quad (1)$$

$$\rho_{nf}\left(\frac{\partial u}{\partial t} + w\frac{\partial u}{\partial z}\right) - 2\Omega v = \mu_{nf}\frac{\partial^2 u}{\partial z^2} + (\rho\beta)_{nf}\, g\,(T - T_\infty) - \frac{\mu_{nf}\, u}{k} - \sigma B_0^2\, u \quad (2)$$

$$\rho_{nf}\left(\frac{\partial v}{\partial t} + w\frac{\partial v}{\partial z}\right) + 2\Omega u = \mu_{nf}\frac{\partial^2 v}{\partial z^2} - \frac{\mu_{nf}\, v}{k} - \sigma B_0^2\, v \quad (3)$$

$$\left(\frac{\partial T}{\partial t} + w\frac{\partial T}{\partial z}\right) = \alpha_{nf}\frac{\partial^2 T}{\partial z^2} - \frac{Q}{(\rho C_\rho)_{nf}}(T - T_\infty) + Q_l\,(C - C_\infty) + \frac{D_m\, K_T}{C_s\,(\rho C_\rho)_{nf}}\frac{\partial^2 C}{\partial z^2} \quad (4)$$

$$\frac{\partial C}{\partial t} + w\frac{\partial C}{\partial z} = D_B\frac{\partial^2 C}{\partial z^2} - K_l\,(C - C_\infty) \quad (5)$$

The thermo-physical properties of the fluids are (Oztop and Abu-Nada [12]),

Table 1: Thermo-physical properties

Physical Properties	Water	Silver (Ag)	Titanium Oxide (TiO_2)
C_p (J/kg K)	4179	235	686.2
ρ (kg/m^3)	997.1	10500	4250
K (W/m K)	0.613	429	8.9538
$\beta\times10^{-5}$ (1/K)	21	1.89	0.9

The boundary conditions for the problem are given by

$$u = 0,\ v = 0,\ T = T_\infty,\ C = C_\infty,\quad t \le 0 \quad (6)$$

$$u = U_0, v = 0, T = T_w + (T_w - T_\infty)\,\varepsilon\, e^{i\omega t},\ C = C_w + (C_w - C_\infty)\,\varepsilon\, e^{i\omega t},\ t > 0 \ \text{ at } \quad z = 0 \quad (7)$$

$$u = 0,\ v = 0,\ T = T_\infty,\ C = C_\infty,\ \text{as} \quad z \to \infty \quad (8)$$

Combining equations (2) and (3), let $q = u + iv$

$$\rho_{nf}\left(\frac{\partial q}{\partial t} + w\frac{\partial q}{\partial z}\right) + 2i\Omega q = \mu_{nf}\frac{\partial^2 q}{\partial z^2} + (\rho\beta)_{nf}\, g\,(T - T_\infty) - \frac{\mu_{nf}\, q}{k} - \sigma B_0^2\, q \quad (9)$$

The following quantities defined as (Abbasi [7, 8]).

$$\rho_{nf} = (1-\phi)\,\rho_f + \phi\rho_s,\ (\rho C_\rho)_{nf} = (1-\phi)(\rho C_\rho)_f + \phi(\rho C_\rho)_s,$$

$$(\rho\beta)_{nf} = (1-\phi)(\rho\beta)_f + \phi(\rho\beta)_s,\ K_{nf} = K_f\left(\frac{K_s + 2K_f - 2\phi(K_f - K_s)}{K_s + 2K_f + 2\phi(K_f - K_s)}\right),$$

$$\mu_{nf} = \frac{\mu_f}{(1-\phi)^{2.5}},\ \alpha_{nf} = \frac{K_{nf}}{(\rho C_\rho)_{nf}}, \quad (10)$$

We consider the solution of Eq. (1) as

$$w = -W_0 \tag{11}$$

Where, the constant $-W_0$ represents the normal velocity at the plate which is positive suction ($W_0 > 0$) and negative for blowing injection ($W_0 < 0$).

Introducing the non-dimensional variables.

$$q^* = \frac{q}{U_0},\ z^* = \frac{U_0 z}{\nu_f}, t^* = \frac{U_0^2 t}{\nu_f}, \omega^* = \frac{\nu_f \omega}{U_0^2}, \theta = \frac{T - T_\infty}{T_w - T_\infty}, \psi = \frac{(C - C_\infty)}{(C_w - C_\infty)}, M^2 = \frac{\sigma B_0^2 \nu_f}{\rho_f U_0^2},$$

$$\mathrm{Du} = \frac{D_m K_T (C_w - C_\infty)}{k_f C_s (T_w - T_\infty)}, Q_L = \frac{Q_l (C_w - C_\infty)}{U_0^2 (T_w - T_\infty)}, \mathrm{Kr} = \frac{K_l \nu_f}{U_0^2}, \mathrm{Pr} = \frac{\nu_f}{\alpha_f}, \mathrm{Sc} = \frac{\nu_f}{D_B},$$

$$R = \frac{2\Omega \nu_f}{U_0^2}, Q^* = \frac{Q \nu^2{}_f}{K_f U_0^2},\ S = \frac{W_0}{U_0}, K = \frac{k \rho_f U_0^2}{\nu_f^2}, \mathrm{Gr} = \frac{(\rho \beta)_f g \nu_f (T_W - T_\infty)}{\rho_f U_0^3}$$

Using non-dimensional variables, the equations (9) and (4) – (5) with the boundary conditions (6) – (8), we get (Dropping asterisks)

$$a_1\left(\frac{\partial q}{\partial t} - S\frac{\partial q}{\partial z}\right) = a_4 \frac{\partial^2 q}{\partial z^2} + a_2 \mathrm{Gr}\,\theta - \left(M^2 + 2iR + \frac{1}{K}\right) q = 0 \tag{12}$$

$$a_3\left(\frac{\partial \theta}{\partial t} - S\frac{\partial \theta}{\partial z} - Q_L \psi\right) = \frac{1}{\mathrm{Pr}}\left(a_5 \frac{\partial^2 \theta}{\partial z^2} - Q\theta\right) + \frac{\mathrm{Du}}{\mathrm{Pr}} \frac{\partial^2 \psi}{\partial z^2} \tag{13}$$

$$\frac{\partial \psi}{\partial t} - S\frac{\partial \psi}{\partial z} = \frac{1}{\mathrm{Sc}}\left(\frac{\partial^2 \psi}{\partial z^2}\right) - \mathrm{Kr}\,\psi \tag{14}$$

With the boundary conditions

$$q = 0,\ \theta = 0, \psi = 0 \quad \text{at} \quad t \le 0 \tag{15}$$

$$q = 1,\ \theta = 1 + \varepsilon e^{i\omega t},\ \psi = 1 + \varepsilon e^{i\omega t},\ \text{at}\ \ t > 0,\ \ z = 0 \tag{16}$$

$$q = 0,\ \theta = 0, \psi = 0 \quad \text{as} \quad z \to \infty \tag{17}$$

To solve the equations (12)-(14) with relevant boundary conditions (16)-(17) with the help of perturbation technique $(\varepsilon << 1)$. The flowing expressions for velocity, temperature and concentration are presumed as

$$q = q_0 + \varepsilon q_1 e^{i\omega t}, \tag{18}$$

$$\theta = \theta_0 + \varepsilon \theta_1 e^{i\omega t}, \tag{19}$$

$$\psi = \psi_0 + \varepsilon \psi_1 e^{i\omega t} \tag{20}$$

Equation (12) - (14) are reduced to

$$a_4 \frac{d^2 q_0}{dz^2} + a_1 S \frac{dq_0}{dz} - \left(M^2 + 2iR + \frac{1}{K} \right) q_0 = -a_2 \,\mathrm{Gr}\, \theta_0 \tag{21}$$

$$a_4 \frac{d^2 q_1}{dz^2} - a_1 S \frac{dq_1}{dz} - \left(M^2 + \frac{1}{K} + i(2R + a_1 \omega) \right) q_1 = -a_2 \,\mathrm{Gr}\, \theta_1 \tag{22}$$

$$a_5 \frac{d^2 \theta_0}{dz^2} - \Pr a_3 S \frac{d\theta_0}{dz} - Q\theta_0 = -\mathrm{Du} \frac{d^2 \psi_0}{dz^2} - \Pr a_3 Q_L \psi_0 \tag{23}$$

$$a_5 \frac{d^2 \theta_1}{dz^2} - \Pr a_3 S \frac{d\theta_1}{dz} - \left(Q + \Pr a_3 i\omega \right) \theta_1 = -\mathrm{Du} \frac{d^2 \psi_1}{dz^2} - \Pr a_3 Q_L \psi_1 \tag{24}$$

$$\frac{d^2 \psi_0}{dz^2} + S\mathrm{Sc} \frac{d\psi_0}{dz} - \mathrm{KrSc}\, \psi_0 = 0 \tag{25}$$

$$\frac{d^2 \psi_1}{dz^2} + S\mathrm{Sc} \frac{d\psi_1}{dz} - \left(i\omega + \mathrm{Kr} \right) \mathrm{Sc}\, \psi_1 = 0 \tag{26}$$

The boundary conditions (16) – (17) become

$$q_0 = 1, \quad q_1 = 0, \quad \theta_0 = 1, \quad \theta_1 = 1, \quad \psi_0 = 1, \quad \psi_1 = 1 \quad \text{at } z = 0 \tag{27}$$

$$q_0 = 0, \quad q_1 = 0, \quad \theta_0 = 0, \quad \theta_1 = 0, \quad \psi_0 = 0, \quad \psi_1 = 0 \quad \text{at } z \to \infty \tag{28}$$

On solving equations (21) – (26) using the boundary conditions (27) - (28), we get

$$q = \left(B_5 e^{-m_5 z} + B_3 e^{-m_3 z} + B_4 e^{-m_1 z} \right) + \varepsilon \left(B_8 e^{-m_6 z} + B_6 e^{-m_4 z} + B_7 e^{-m_2 z} \right) e^{i\omega t} \tag{29}$$

$$\theta = \left(B_1 e^{-m_3 z} + A_1 e^{-m_1 z} \right) + \varepsilon \left(B_2 e^{-m_4 z} + A_2 e^{-m_2 z} \right) e^{i\omega t} \tag{30}$$

$$\psi = \left(e^{-m_1 z} \right) + \varepsilon \left(e^{-m_2 z} \right) e^{i\omega t} \tag{31}$$

The skin friction, Nusselt number and Sherwood number at the plate in dimensional form are,

$$\tau = \left(\frac{\partial q}{\partial z} \right)_{z=0}, \; Nu = -\left(\frac{\partial \theta}{\partial z} \right)_{z=0} \text{ and } Sh = -\left(\frac{\partial \psi}{\partial z} \right)_{z=0} \tag{32}$$

3. Results and Discussion

The results are presented in Figs.2–10 and in Tables 2–4. The effects of flow parameters on velocity, temperature and concentration of nano-particles, the skin friction, the rate of heat and mass transfer coefficients have been discussed computationally. We have chosen for velocity and skin friction $\varepsilon = 0.001, \omega = \pi/6, \Pr = 6.2, Q = 2, \mathrm{Sc} = 0.6$, while the remaining parameters are varied over a range. **Figs.2** present the velocity profiles of *u* and *v* with Hartmann number *M* for the nano-particles Ag and TiO_2. Both velocities *u* and *v* decelerates with increasing *M*. Since the consequences of a transverse magnetic field provide climb to a resistive-type force called the Lorentz force. Also from **Figs.3**, it is observed that the nanofluid velocity increases by increasing K. Minor the permeability lesser the fluid speed is scrutinized in entire fluid region. Similar behaviour is observed for increasing Grashof number Gr (**Figs.4**). It is illustrated from **Figs.5** that the boundary layer thickness increases with Du for both nano-fluids. Thus the hydrodynamic boundary layer thickness increases as the Dufour number increases. It is determined from **Figs.6** that the velocity increase with increase of Q_L. Since, the buoyancy force accelerates the flow while heat is absorbed. Supremacy of conduction over radiation absorption is increasing thickness of the momentum boundary layer.

From **Figs.7,** the velocity of the fluid across the boundary layer decreases by increasing the suction parameter S. The maximum velocity of Ag–water nano-fluid is higher than that of the TiO_2–water nano-fluid accomplished at vicinity of the plate. The magnitude of the velocity components u and v reduces with increasing rotation parameter R (**Figs.8)**.

Figs. 9 depict the temperature profiles against parameters Du, Q_L and S for both nano-fluids. Du causes to augment the thermal boundary layer thickness. Physically, decreasing Du clearly retards the influence of species gradients on the temperature, Hence temperature is lessens and the boundary layer thickness cooled. The temperature increase with increase of Q_L. Since, when heat is absorbed, the buoyancy force accelerates the flow. The temperature increases with increasing S at the vicinity of the boundary later it retards during the fluid region.

The concentration boundary layer of the flow is shown in **Figs. 10.** As the suction parameter increases the species concentration reduces and then the solutal boundary layer thickness decreases. Since, the suction stabilizes the boundary growth. An increase in Kc reduces the concentration. The parameter Kc is to decrease in the chemical molecular diffusivity.

The arithmetical values of the Skin-friction and Nusselt number for the nano-particles Ag and TiO_2 are presented in Tables 2 and 3, and Sherwood number are presented in the Table 4. From Table 2, the skin friction increases with the increasing values of Gr, K, Q_L and Du, and reduces with M, R and S for both the nano-particles Ag and TiO_2. From Table 3, the Nusselt number increases with S, Du and Q_L for both the nano-particles Ag and TiO_2. From Table 4 it is clear that the Sheerwood number increases with the increasing values of S and Kr. It decreases with increasing time. The results are good agreement with the results of Hamad and Pop [13] (Table 5).

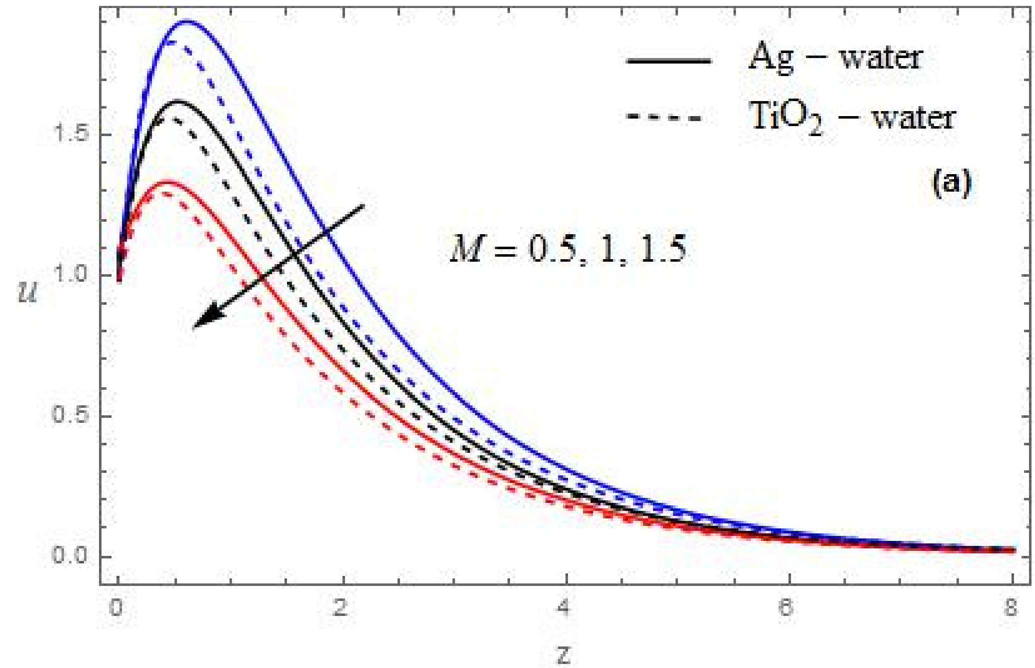

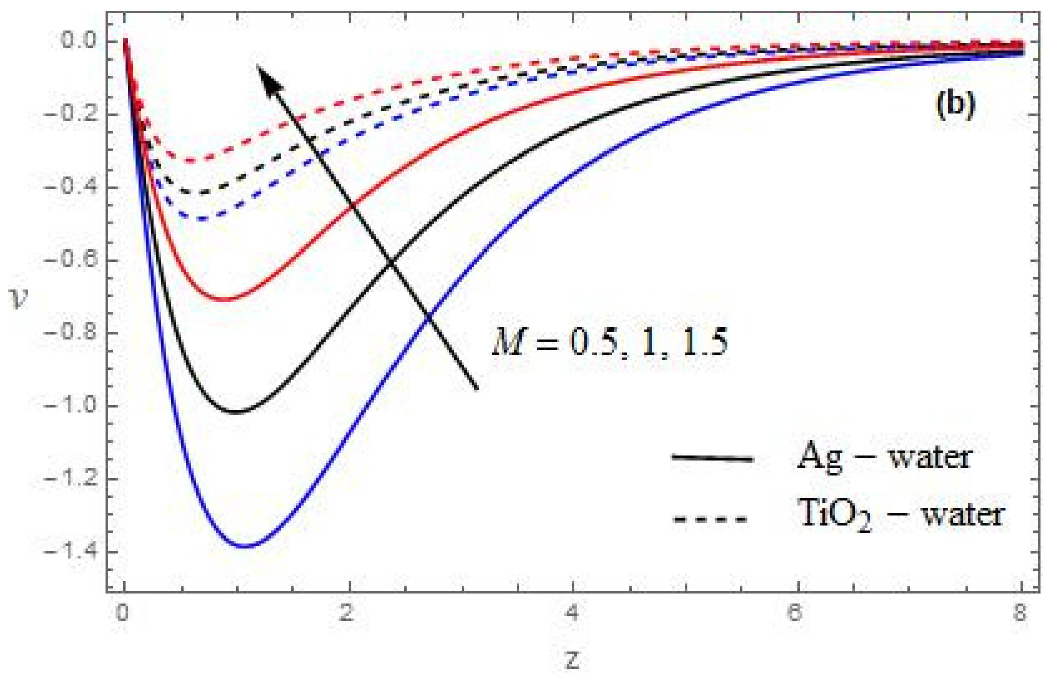

Figs. 2 (a-b) The velocity profiles against M with
$K = 0.5, S = 1, \mathrm{Du} = 1, \mathrm{Gr} = 3, Q_L = 1, R = 0.5$

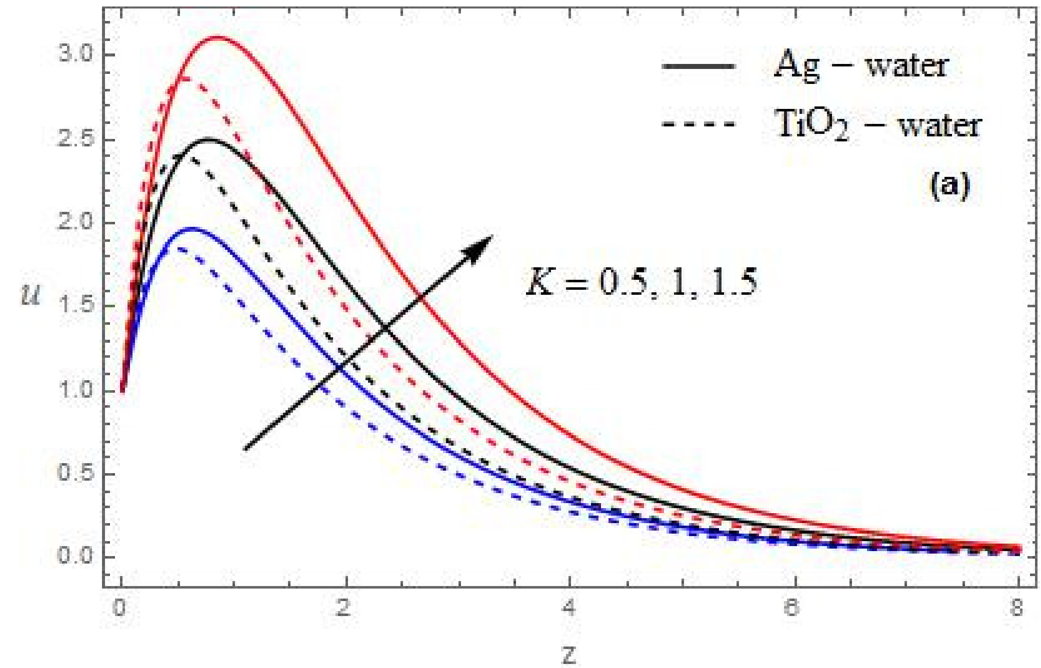

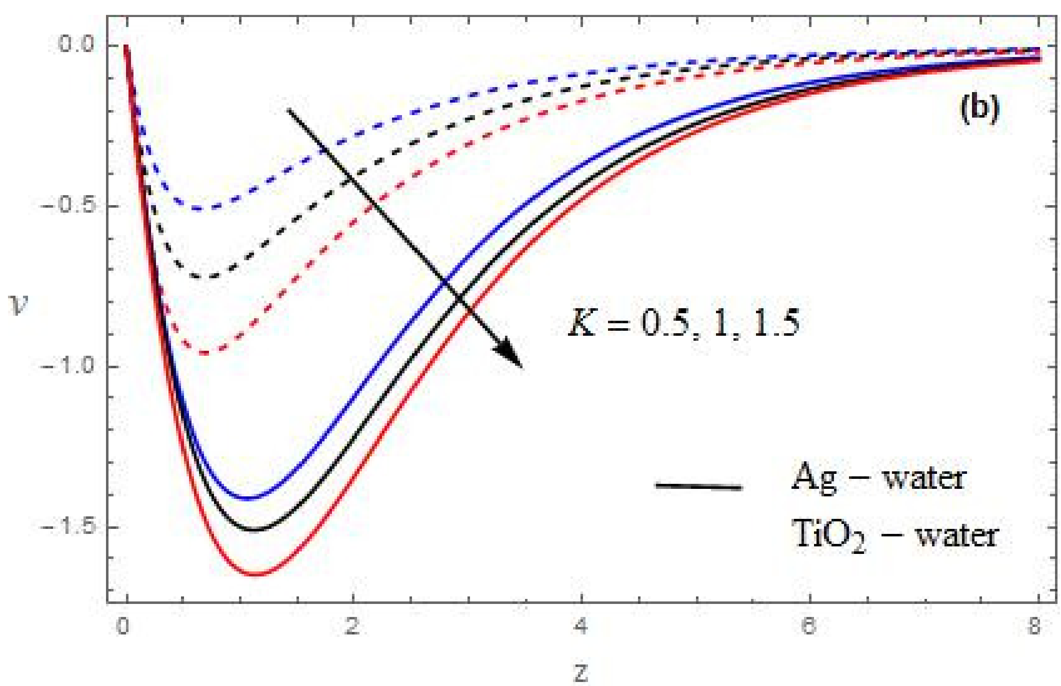

Figs. 3 (a-b) The velocity profiles against K with
$M = 0.5, S = 1, \mathrm{Du} = 1, \mathrm{Gr} = 3, Q_L = 1, R = 0.5$

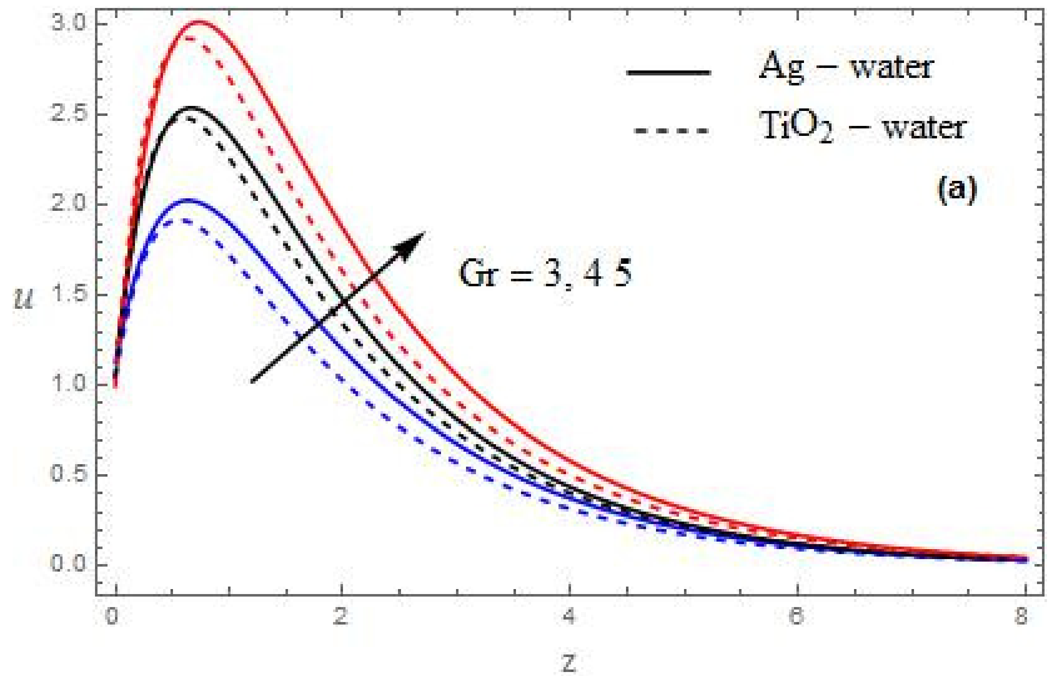

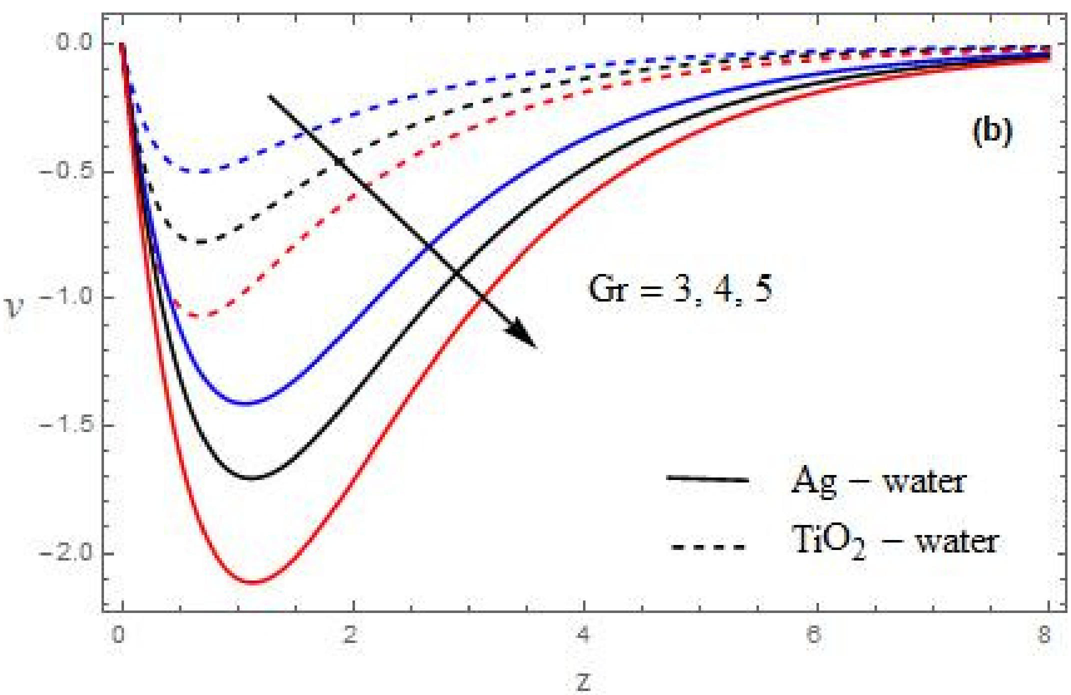

Figs. 4 (a-b) The velocity profiles against Gr with
$M = 0.5, K = 0.5, S = 1, \mathrm{Du} = 1, Q_L = 1, R = 0.5$

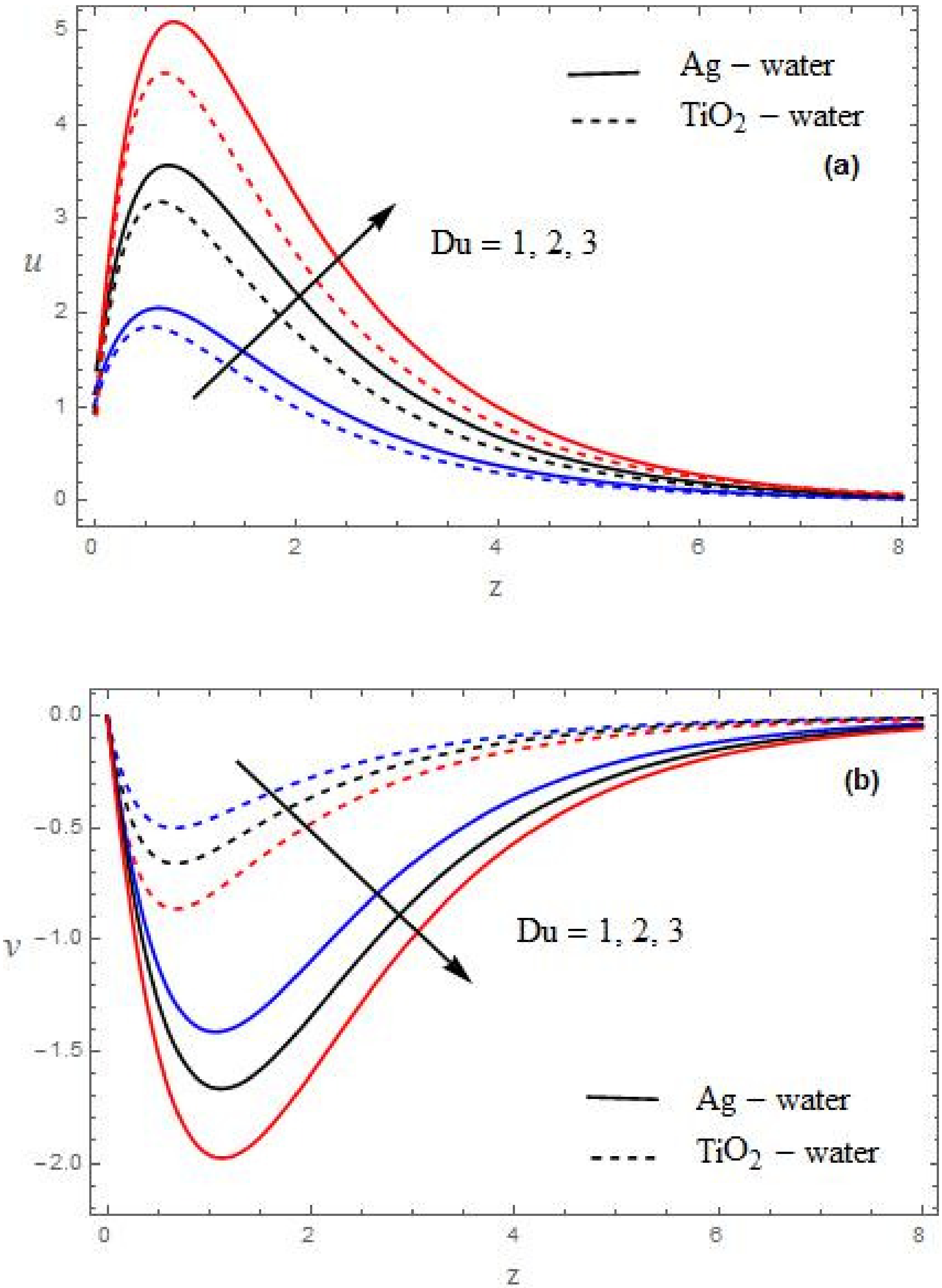

Figs. 5 (a-b) The velocity profiles against Du with
$M = 0.5, K = 0.5, S = 1, \mathrm{Gr} = 3, Q_L = 1, R = 0.5$

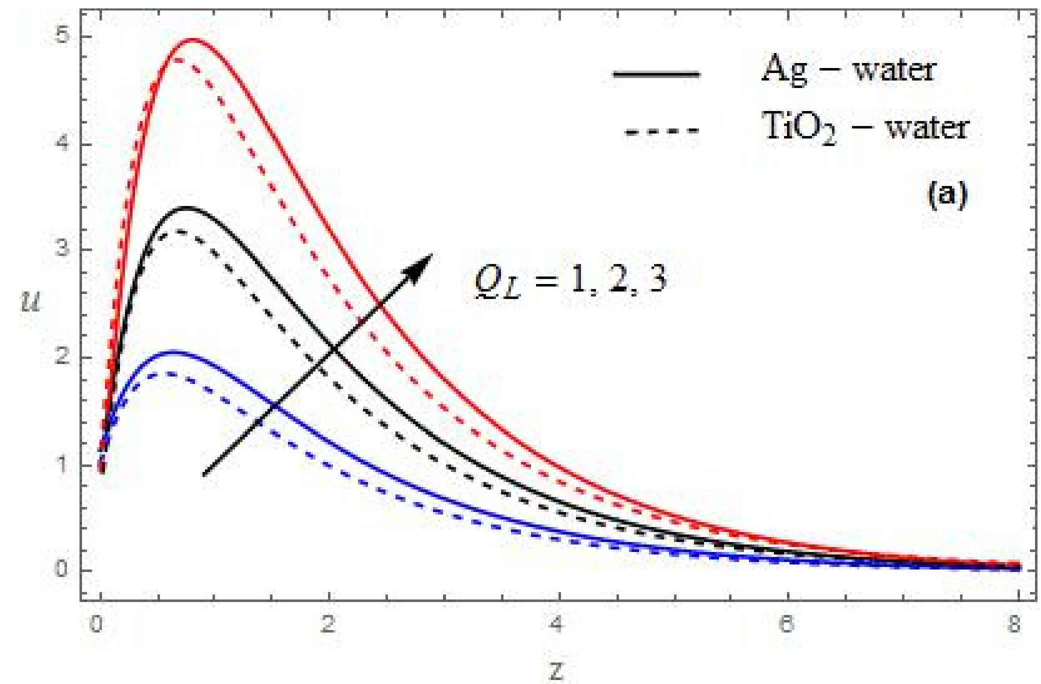

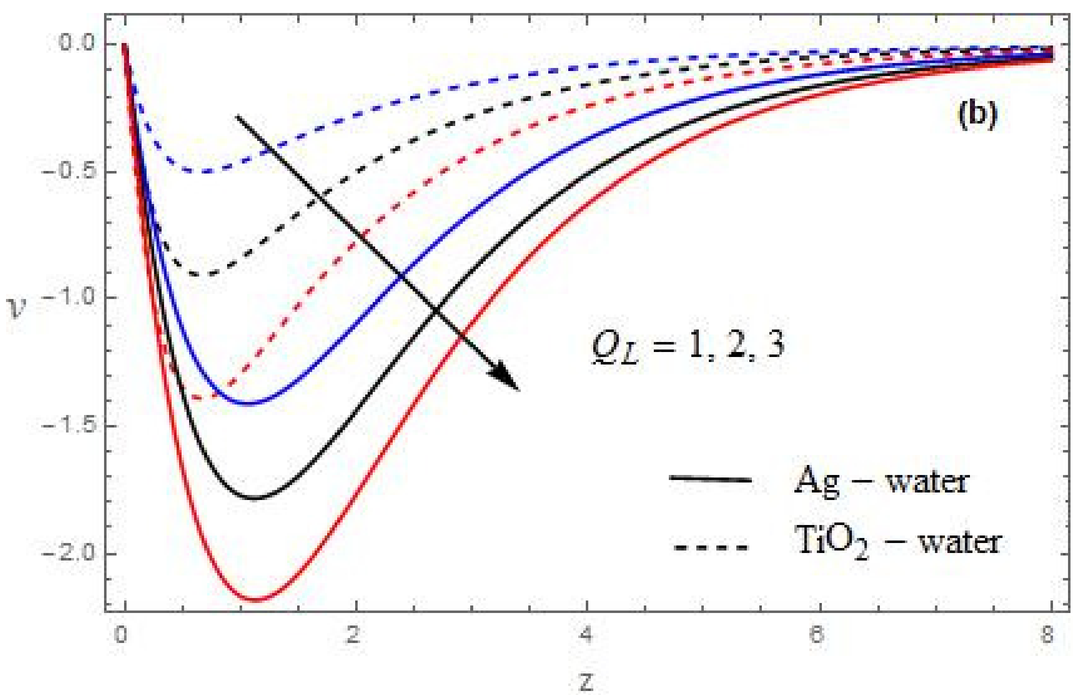

Figs. 6 (a-b) The velocity profiles against Q_L with
$M = 0.5, K = 0.5, S = 1, \mathrm{Du} = 1, \mathrm{Gr} = 3, R = 0.5$

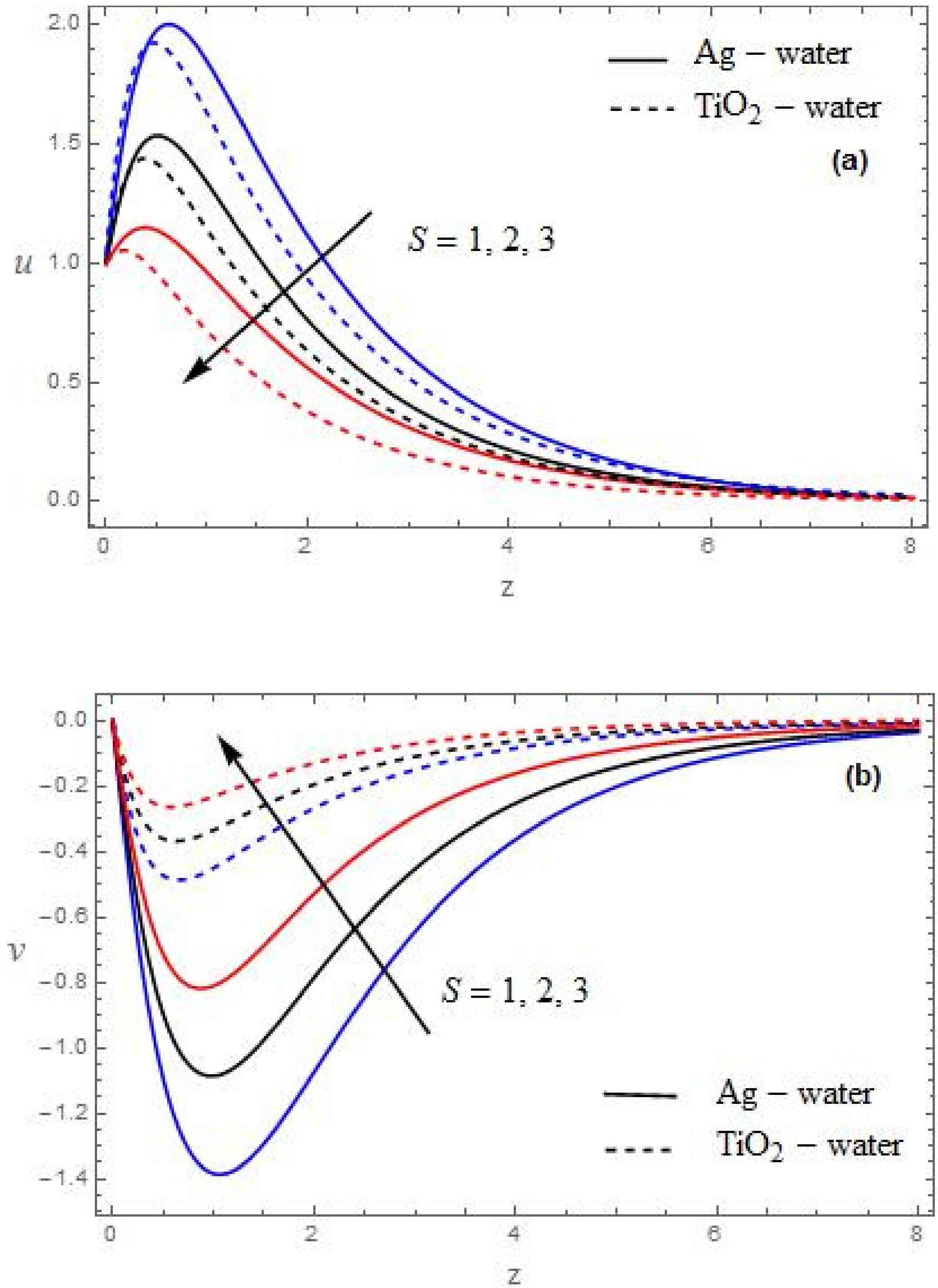

Figs. 7 (a-b) The velocity profiles against S with
$M = 0.5, K = 0.5, \mathrm{Du} = 1, \mathrm{Gr} = 3, Q_L = 1, R = 0.5$

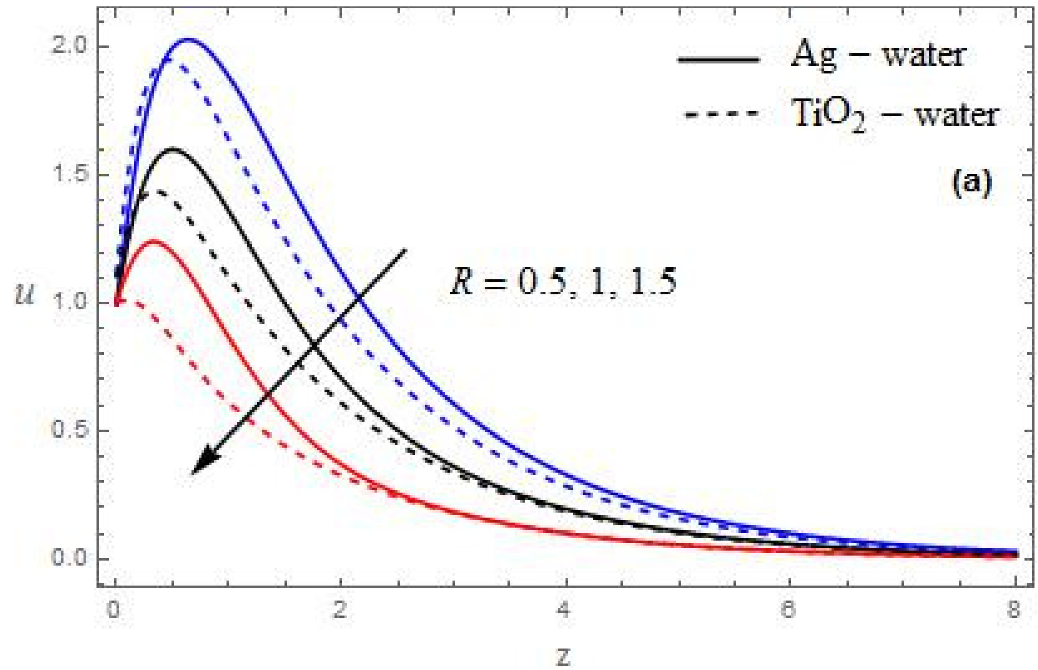

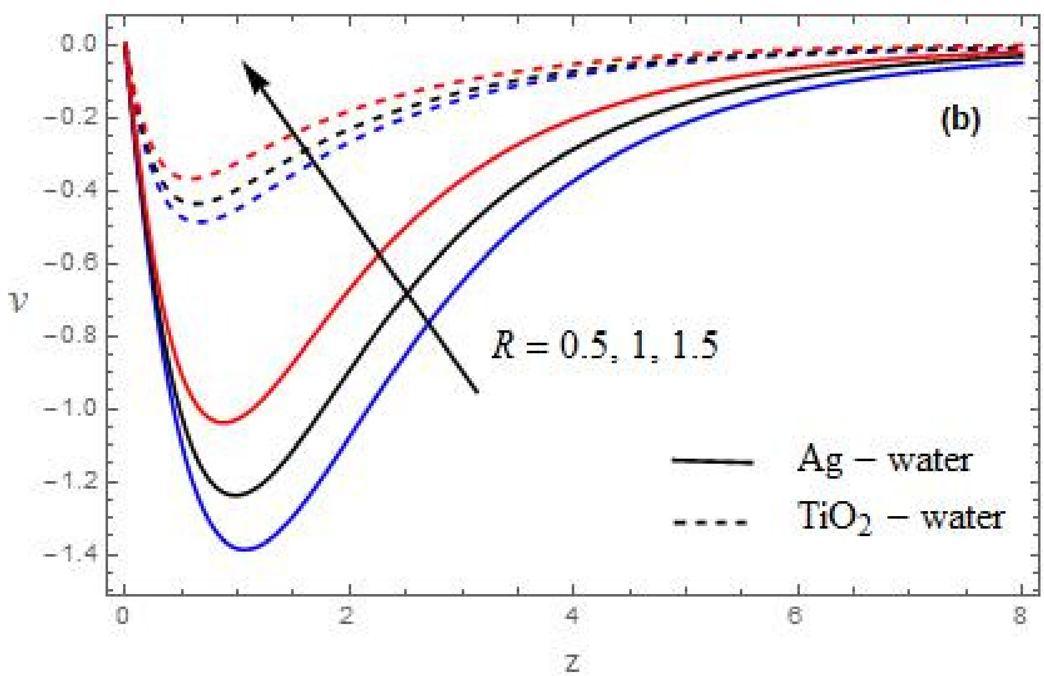

Figs. 8 (a-b) The velocity profiles against R with
$M = 0.5, K = 0.5, \mathrm{Du} = 1, \mathrm{Gr} = 3, Q_L = 1, S = 1$

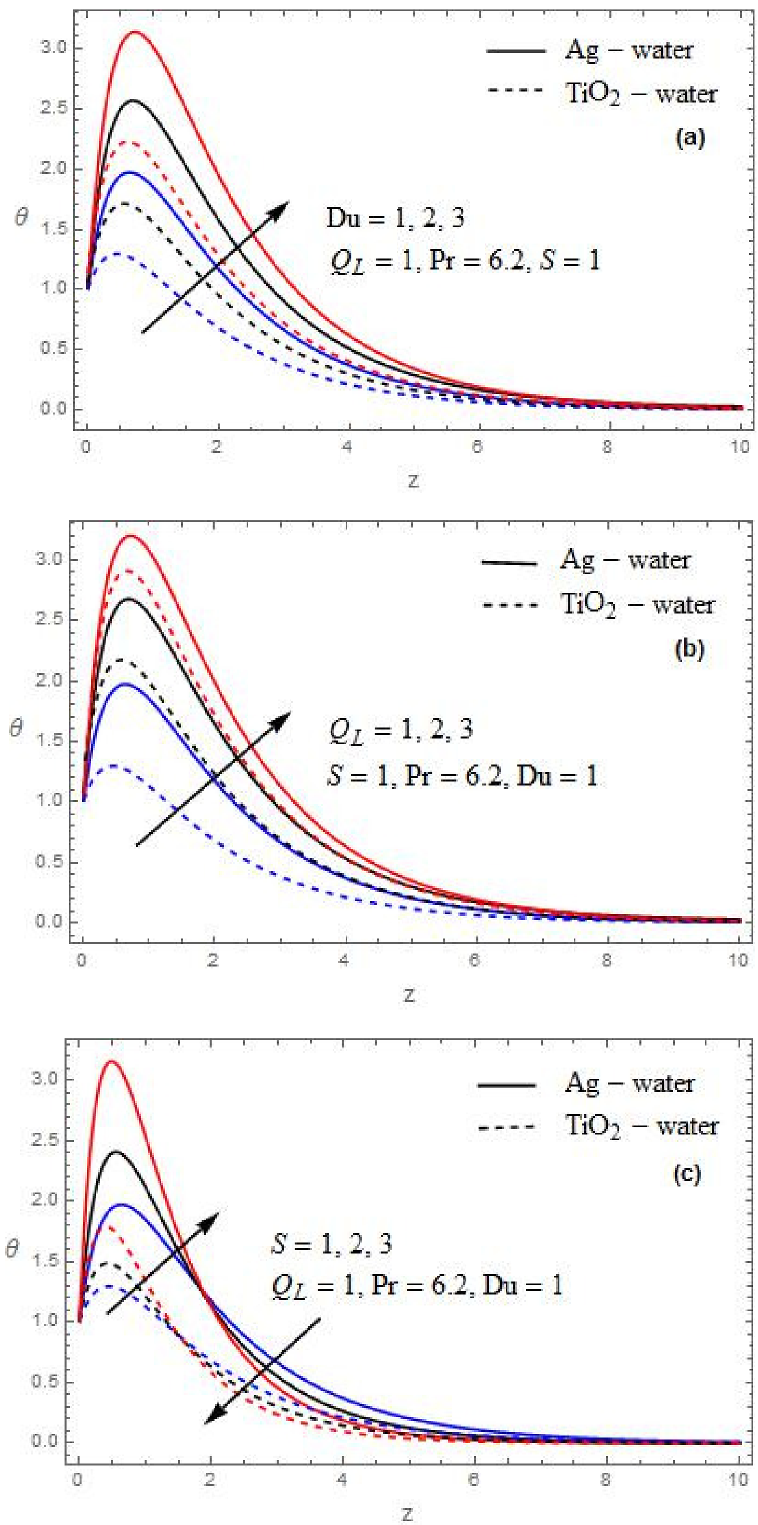

Figs. 9 (a-c) Temperature profiles with Du, Q_L and S

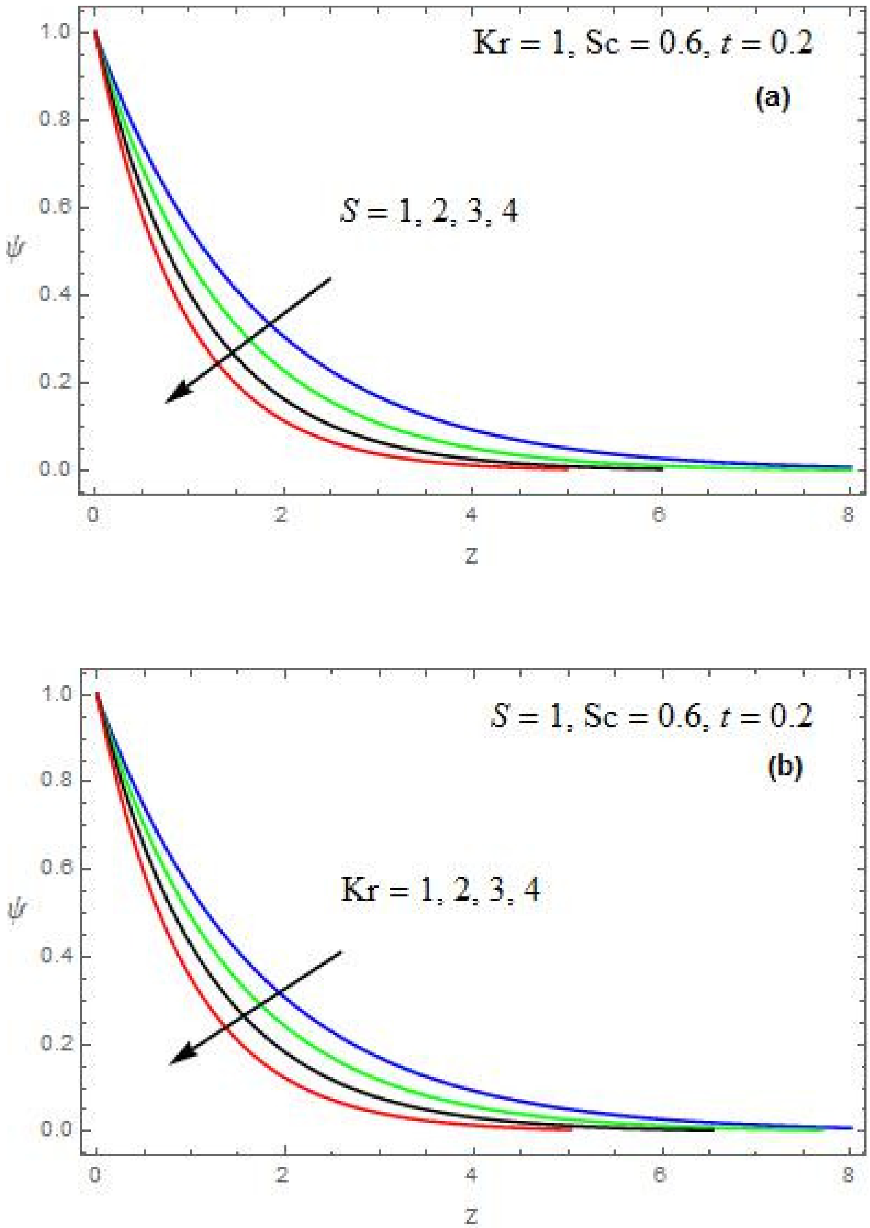

Figs. 10 (a-b) Concentration Profiles with *S* and Kr

Table 2. Skin friction

M	K	Gr	Du	Q_L	S	R	Ag	TiO_2
0.5	0.5	3	1	1	1	0.5	4.53069	2.87534
1							3.27517	1.98690
1.5							1.71728	0.94951
	1						7.06758	4.77792
	1.5						8.30973	5.81166
		4					7.27314	4.57277
		5					10.0156	6.27021
			2				4.91159	3.10621
			3				5.29249	3.33709
				2			11.9883	7.42058
				3			19.4458	11.9658
					2		-3.15995	-0.99983
					3		-7.74871	-2.98103
						1	4.32566	2.52415
						1.5	4.01552	2.20144

Table 3. Nusselt number

Du	S	Q_L	Ag	TiO_2
1	1	1	-4.01310	-3.99051
2			-6.08865	-6.05172
3			-8.16420	-8.11294
	2		-6.78362	-6.62399
	3		-12.0353	-11.4432
		2	-8.13860	-8.11003
		3	-12.2641	-12.2296

Table 4. Sherwood number

S	Kr	t	Sh
1	1	0.2	0.592358
2			0.738807
3			0.904395
	2		0.783158
	3		0.930737
		0.4	0.592336
		0.6	0.592308

Table 5. Comparison of the results for Nusselt number ($\mathrm{Du} = Q_L = 0$)

S	Q	Ag Hamad and Pop [13]	Ag Present results	TiO_2 Hamad and Pop [13]	TiO_2 Present results
1	1	2.18785	2.18795	2.19010	2.19022
2		2.63198	2.63207	2.63710	2.63728
3		3.13033	3.13043	3.13899	3.13910
	2	2.92694	2.92702	2.92909	2.92919
	3	3.49707	3.49719	3.49921	3.49932

4. Conclusions

For the nano-particles Ag and TiO_2

1. The resultant velocity diminishes with increasing M, S and R, while it amplifies with Q_L and Du.
2. Q_L and Du lead to increase the thermal boundary layer thickness.
3. The concentration reduces with increase in S or Kc.
4. The skin friction coefficient augments with the increasing Gr, K, Q_L and Du.
5. Nu decreases with S, Du and Q_L.
6. *Sh* increases with S and Kr.

Appendix:

$$a_1 = \left((1-\phi) + \phi \left(\frac{\rho_s}{\rho_f} \right) \right),$$

$$a_2 = \left((1-\phi) + \phi \left(\frac{(\rho\beta)_s}{(\rho\beta)_f} \right) \right),$$

$$a_3 = \left((1-\phi) + \phi \left(\frac{(\rho C_p)_s}{(\rho C_p)_f} \right) \right),$$

$$a_4 = \frac{1}{(1-\phi)^{2.5}},$$

$$a_5 = \frac{k_{nf}}{k_f} = \left(\frac{(1+2\phi)+(2-2\phi)\left(\frac{K_f}{K_s}\right)}{(1-2\phi)+(2+2\phi)\left(\frac{K_f}{K_s}\right)} \right),$$

$$A_1 = -\left(\frac{m_1^2 \mathrm{Du} + \Pr Q_L a_3}{a_5 m_1^2 - \Pr a_3 S m_1 - Q} \right),$$

$$A_2 = -\left(\frac{m_2^2 \mathrm{Du} + \Pr Q_L a_3}{a_5 m_2^2 - \Pr a_3 S m_2 - (Q + i\omega \Pr a_3)} \right),$$

$$B_1 = 1 - A_1,$$

$$B_2 = 1 - A_2,$$

$$B_3 = -\left(\frac{a_2 B_1 \mathrm{Gr}}{a_4 m_3^2 - a_1 S m_3 - \left(M^2 + 2iR + (1/K)\right)} \right),$$

$$B_4 = -\left(\frac{a_2 A_1 \mathrm{Gr}}{a_4 m_1^2 - a_1 S m_1 - \left(M^2 + 2iR + (1/K)\right)} \right),$$

$$B_5 = (1 - B_3 - B_4),$$

$$B_6 = -\left(\frac{a_2 B_2 \mathrm{Gr}}{a_4 m_4^2 - a_1 S m_4 - \left(M^2 + (1/K) + i(2R + a_1\omega)\right)} \right),$$

$$B_7 = -\left(\frac{a_2 A_2 \mathrm{Gr}}{a_4 m_2^2 - a_1 S m_2 - \left(M^2 + (1/K)\right) + i(2R + a_1\omega)} \right),$$

$$B_8 = -(B_6 + B_7),$$

$$m_1 = \frac{S\mathrm{Sc} + \sqrt{(S\mathrm{Sc})^2 + 4\mathrm{KrSc}}}{2},$$

$$m_2 = \frac{S\mathrm{Sc} + \sqrt{(S\mathrm{Sc})^2 + 4\mathrm{Sc}(i\omega + \mathrm{Kr})}}{2},$$

$$m_3 = \frac{\Pr a_3 S + \sqrt{(\Pr a_3 S)^2 + 4 a_5 Q}}{2},$$

$$m_4 = \frac{\Pr a_3 S + \sqrt{(\Pr a_3 S)^2 + 4a_5 (Q + i\omega \Pr a_3)}}{2a_5},$$

$$m_5 = \frac{a_1 S + \sqrt{(a_1 S)^2 + 4a_4 (M^2 + (1/K) + 2iR)}}{2a_4},$$

$$m_6 = \frac{a_1 S + \sqrt{(a_1 S)^2 + 4a_4 \left(a_1 i\omega + \left(M^2 + (1/K) + 2iR\right)\right)}}{2a_4}$$

References

[1]. Choi S. Enhancing thermal conductivity of fluids with nanoparticle.In: Siginer DA, Wang HP, editors, Developments and applications of non-newtonian flows, vol. 66, American Society of Mathematical Engineers, New York; 1995. p. 99–105.

[2]. Ablel-Rahman, G.M. (2008) Thermal Diffusion and MHD Effects on Combined Free Forced Convection and Mass Transfer Flow of a Viscous Fluid Flow through a Porous Medium with Heat Generation. *Chemical Engineering and Technology*, 31, 554-559. http://dx.doi.org/10.1002/ceat.200700487

[3]. Reddy, N.A., Raju, M.C. and Varma, S.V.K. (2009) Thermo Diffusion and Chemical Effects with Simultaneous Thermal and Mass Diffusion in MHD Mixed Convection Flow with Ohmic Heating. *Journal of Naval Architecture and Marine Engineering*, 6, 84-93.

[4]. Sarma, D., Ahmed, N. and Deka, H. (2014) MHD Free Convection and Mass Transfer Flow past an Accelerated Vertical Plate with Chemical Reaction in Presence of Radiation. *Latin American Applied Research*, 44, 1-8.

[5]. Ahmed, S. and Batin, A. (2014) Magnetohydrodynamic Heat and Mass Transfer Flow with Induced Magnetic Field and Viscous Dissipative Effects. *Latin American Applied Research*, 44, 9-17.

[6]. Mutuku-Njane, W.N. and Makinde, O.D. (2014) On Hydromagnetic Boundary Layer Flow of Nanofluids over a Permeable Moving Surface with Newtonian Heating. *Latin American Applied Research*, **44**, 57-62.

[7]. Abbasi FM, Hayat T, Alsaadi F. Peristaltic transport of magnetonanoparticles submerged in water: model for drug delivery system. Physica E 2015;68:123–32.

[8]. Abbasi FM, Hayat T, Alsaadi F. Hydromagnetic peristaltic transport of water-based nanofluids with slip effects through an asymmetric channel. Int J Mod Phys B 2015;29:1–17.

[9]. Veera Krishna.M, G.Subba Reddy, A.J.Chamkha, "Hall effects on unsteady MHD oscillatory free convective flow of second grade fluid through porous medium between two vertical plates," Physics of Fluids, **30**, 023106 (2018). doi: 10.1063/1.5010863

[10]. Veera Krishna.M, A.J.Chamkha, Hall effects on unsteady MHD flow of second grade fluid through porous medium with ramped wall temperature and ramped surface concentration, Physics of Fluids **30**, 053101 (2018), doi: 10.1063/1.5025542

[11]. Veera Krishna.M, A.J.Chamkha, Hall Effects on MHD Squeezing Flow of A Water-based Nanofluid between two Parallel disks, Journal of Porous media, 21(13), pp. 1345–1359 (2018). DOI: 10.1615/JPorMedia.2018028721

[12]. Oztop HF, Abu-Nada E. Numerical study of natural convection in partially heated rectangular enclosures filled with nanofluids. Int. J. Heat Mass Transf. 29, pp. 1326–1336, 2008.

[13]. Hamad. M.A.A., Pop.I., Unsteady MHD free convection flow past a vertical permeable flat plate in a rotating frame of reference with constant heat source in a nanofluid, Heat and mass transfer, 47, pp. 1517-1524 (2011). DOI 10.1007/s00231-011-0816-6.

[14]. Veera Krishna.M., M.Gangadhar Reddy, MHD Free Convective Boundary Layer Flow through Porous medium Past a Moving Vertical Plate with Heat Source and Chemical Reaction, Materials Today: Proceedings, vol. 5, pp. 91–98, 2018. https://doi.org/10.1016/j.matpr.2017.11.058.

[15]. Veera Krishna.M., G.Subba Reddy, MHD Forced Convective flow of Non-Newtonian fluid through Stumpy Permeable Porous medium, Materials Today: Proceedings, vol. 5, pp. 175–183, 2018. https://doi.org/10.1016/j.matpr.2017.11.069.

[16]. Krishna.M.V., Kamboji Jyothi, Hall effects on MHD Rotating flow of a Visco-elastic Fluid through a Porous medium Over an Infinite Oscillating Porous Plate with Heat source and Chemical reaction, Materials Today: Proceedings, vol. 5, pp. 367–380, 2018. https://doi.org/10.1016/j.matpr.2017.11.094.

[17]. Krishna, M.V., Jyothi, K., Chamkha, A.J., Heat and mass transfer on MHD flow of second-grade fluid through porous medium over a semi-infinite vertical stretching sheet, Journal of Porous media, 23(8), pp. 751-765, 2020.

[18]. VeeraKrishna.M., B.V.Swarnalathamma, Convective Heat and Mass Transfer on MHD Peristaltic Flow of Williamson Fluid with the Effect of Inclined Magnetic Field," AIP Conference Proceedings, vol. 1728, p. 020461, 2016. DOI: 10.1063/1.4946512

[19]. Swarnalathamma. B. V., M. Veera Krishna, Peristaltic hemodynamic flow of couple stress fluid through a porous medium under the influence of magnetic field with slip effect AIP Conference Proceedings, vol. 1728, p. 020603, 2016. DOI: 10.1063/1.4946654.

[20]. VeeraKrishna.M., M.Gangadhar Reddy MHD free convective rotating flow of Visco-elastic fluid past an infinite vertical oscillating porous plate with chemical reaction, IOP Conf. Series: Materials Science and Engineering, vol. 149, p. 012217, 2016 DOI: 10.1088/1757-899X/149/1/012217.

[21]. VeeraKrishna.M., G.Subba Reddy Unsteady MHD convective flow of Second grade fluid through a porous medium in a Rotating parallel plate channel with temperature dependent source, IOP Conf. Series: Materials Science and Engineering, vol. 149, p. 012216, 2016. DOI**:** 10.1088/1757-899X/149/1/012216.

[22]. Veera Krishna.M., B.V.Swarnalathamma and J. Prakash, "Heat and mass transfer on unsteady MHD Oscillatory flow of blood through porous arteriole, Applications of Fluid Dynamics, Lecture Notes in Mechanical Engineering, vol. XXII, pp. 207-224, 2018. Doi: 10.1007/978-981-10-5329-0_14.

[23]. Sadiq Basha PM, Krishna M.V., Nagarathna N. Hall and ion slip effects on steady MHD free convective flow through a porous medium in a vertical microchannel. Heat Transfer. 2020;1–17. https://doi.org/10.1002/htj.21826

[24]. Veera Krishna, M., Chamkha, A.J., Hall and ion slip effects on MHD rotating boundary layer flow of nanofluid past an infinite vertical plate embedded in a porous medium, Results in Physics, 15, 102652, 2019. DOI: https://doi.org/10.1016/j.rinp.2019.102652

[25]. Veera Krishna, M., Swarnalathamma, B.V., Chamkha, A.J., Investigations of Soret, Joule and Hall effects on MHD rotating mixed convective flow past an infinite vertical porous plate, Journal of Ocean Engineering and Science, 4(3), pp. 263-275, 2019. DOI: https://doi.org/10.1016/j.joes.2019.05.002.

[26]. Veera Krishna.M., Chamkha, A.J., Hall effects on MHD Squeezing flow of a water based nano fluid between two parallel disks, Journal of Porous media, 22(2), pp. 209-223, 2019. **DOI:** https://doi.org/10.1615/JPorMedia.2018028721

[27]. Veera Krishna. M., Chamkha, A.J., Hall and ion slip effects on Unsteady MHD Convective Rotating flow of Nanofluids - Application in Biomedical Engineering, Journal of Egyptian Mathematical Society, 28(1), pp. 1-14, 2020. https://doi.org/10.1186/s42787-019-0065-2

[28]. Veera Krishna.M., Heat transport on steady MHD flow of copper and alumina nanofluids past a stretching porous surface, Heat Transfer, 49(3), 1374-1385, 2020, doi: https://doi.org/10.1002/htj.21667

[29]. Veera Krishna, M., Ameer Ahamad, N., Chamkha, A.J., Hall and ion slip effects on unsteady MHD free convective rotating flow through a saturated porous medium over an exponential accelerated plate, Alexandria Engineering Journal, 59, 565-577, 2020 https://doi.org/10.1016/j.aej.2020.01.043

[30]. Veera Krishna, M., Sravanthi, C.S., Gorla, R.S.R., Hall and ion slip effects on MHD rotating flow of ciliary propulsion of microscopic organism through porous media, International Communications in Heat and Mass Transfer, 112, 104500, 2020. https://doi.org/10.1016/j.icheatmasstransfer.2020.104500

[31]. Veera Krishna, M., Chamkha, A.J., Hall and ion slip effects on MHD rotating flow of elastico-viscous fluid through porous medium, International Communications in Heat and Mass Transfer, 113, 104494, 2020. https://doi.org/10.1016/j.icheatmasstransfer.2020.104494

[32]. Veera Krishna, M., Hall and ion slip effects on MHD free convective rotating flow bounded by the semi-infinite vertical porous surface, Heat Transfer, 49(4), 1920–1938, 2020. https://doi.org/10.1002/htj.21700

[33]. Veera Krishna, M., Hall and ion slip effects on MHD laminar flow of an elastic-viscous (Walter's-B) fluid, Heat Transfer, 49(4), 2311–2329, 2020. https://doi.org/10.1002/htj.21722